

Synchronous reluctance machine drive control with fast prototyping card implementation

WOJCIECH BURLIKOWSKI^{ORCID}, PAWEŁ KIELAN^{ORCID}, ZYGMUNT KOWALIK^{ORCID}

Department of Mechatronics, Faculty of Electrical Engineering

Silesian University of Technology

Akademicka 10A, 44-100 Gliwice, Poland

e-mails: {wojciech.burlikowski/pawel.kielan/zygmunt.kowalik}@polsl.pl

(Received: 20.03.2020, revised: 29.05.2020)

Abstract: The Synchronous Reluctance Machine (SynRM) is an electrical machine in which the useful electromagnetic torque is produced due to rotor saliency. Its high power- and torque-to-mass ratio and very good efficiency make it a cheap and simple alternative for permanent magnet or induction motors, e.g. in electromobility applications. However, because of magnetic nonlinearities, the rotational speed and torque control of a SynRM is a nontrivial task. In the paper, a control algorithm based on a Hamiltonian mathematical model is presented. The model is formulated using measurement results, obtained by the drive controller. An algorithm is tested in the drive system consisting of a SynRM with the classical rotor and a fast prototyping card. The drive dynamic response in transient states is very good, but the proposed algorithm does not ensure the best efficiency after steady state angular velocity is achieved.

Key words: direct torque control, fast prototyping card, Hamiltonian machine model, synchronous reluctance motor

1. Introduction

During previous several years an increased attention of the electric machine industry has been focused on the so called Synchronous Reluctance Motor (SynRM). It is a result of intense research and development of high-torque SynRM's rotor designs (Fig. 1(c)) surpassing induction motors in terms of efficiency and robustness [1, 2], especially when its construction incorporates assisting permanent magnets [3]. Although nowadays the SynRMs are mostly used in less demanding applications (e.g. driving pumps or fans), there are new designs and control strategies developed which enable the use of these motors in electrical cars [4, 5], traction vehicles [6] or even bicycles [7].



© 2020. The Author(s). This is an open-access article distributed under the terms of the Creative Commons Attribution-NonCommercial-NoDerivatives License (CC BY-NC-ND 4.0, <https://creativecommons.org/licenses/by-nc-nd/4.0/>), which permits use, distribution, and reproduction in any medium, provided that the Article is properly cited, the use is non-commercial, and no modifications or adaptations are made.

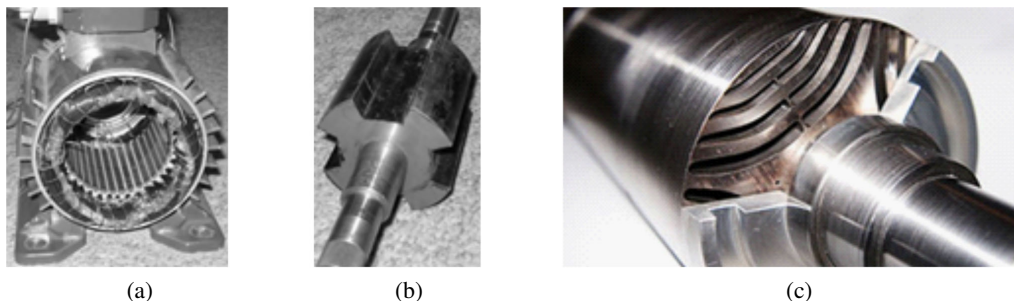


Fig. 1. Main parts of SynRM: (a) stator; (b) classical rotor; (c) modern rotor. (a) and (b) show the parts of the prototype SynRM machine that is a component of the proposed SynRM drive system

The perspective of application of the SynRM, since its first practical design proposed by Kostko in 1923, was not very optimistic as it was regarded merely as a special case of synchronous machine [8]. Kostko himself expressed it in the following statement: “... *it can hardly be expected that reaction motors will ever be extensively used*”. The main reason of these doubts was a difficult starting and control of the SynRM which was not solved until the 1970s with the introduction of microprocessor controlled power converters [9]. Another challenge for control of the SynRM was its very nonlinear operational characteristics resulting from saturation of its magnetic circuit and its poor performance in the case of the classical design of the rotor (Fig. 1(b)) which changed recently with the introduction of modern rotor designs (Fig. 1(c)). The optimization of the magnetic circuit of SynRMs was the scope of many recent works e.g. to achieve better power factor [10], lessen torque ripples [11] or to elevate the general performance of the machine [12].

The other way of improving the SynRM drive features is to improve its control. Generally, methods used to control the SynRM, being the topic of the paper, are very similar like in the case of all synchronous machines (e.g. Permanent Magnet Synchronous Machines [13]). Therefore these methods are defined for a two-axis dq model of a generalized synchronous machine proposed in the 1920s by Park [14]. They belong to the so called Vector Control (VC) methods which can be briefly divided into two main classes.

Control algorithms of the first class incorporate simple, linear mathematical models of a machine and solve the problem of nonlinearity using robust methods of control (fuzzy logic, neural networks, etc.) [15, 16]. That approach to its control gives good results, but usually demands faster microcontrollers for handling the algorithm computations and does not give insight into the operation of the controlled machine.

The opposite approach is to use a more precise mathematical model of the controlled machine, but much simpler control algorithms. Such an approach is present in the literature since the early 90s [9, 17], but recently got more interest due to the introduction of model predictive control [18, 19]. In this type of control algorithm a state of the machine in the given state space is found, usually followed by the linearization of it in the assumed region and acting accordingly to the linearized model. Much work is also focused on the so called sensorless algorithms, in which the angular position of the rotor of the machine (required in VC algorithms) is estimated rather than measured [19, 20]. Such an approach simplifies the hardware of the drive system but complicates the control algorithm and signal processing. a very interesting approach is also introduced in

[13] to control the permanent magnet assisted SynRM, based on the characteristic of flux linkage values with respect to currents in the winding of the machine. This characteristic is obtained using the results of measurements performed with a constant angular velocity of the machine, which makes it necessary to use an additional machine as a load.

The authors of this paper believe, that control algorithms based on mathematical models introduce better possibilities to optimize the operation of a specific machine due to precise observation and control of its state. This is especially important when the behavior of the controlled machine is nonlinear. However, such an approach requires accurate mathematical models and numerical data that specifies it. The issues of obtaining and handling such models and data are still subjects of debate. In the paper, an algorithm for controlling an electrical machine using its Hamiltonian model, based on the function of flux linkages with respect to current values, is presented. In the case of the SynRM control such a model could be more suitable than the more widely used Lagrangian model, based on dynamical inductance values [21]. The aim of the work is to implement the algorithm in the prototype drive system. The mathematical model of the machine, that is used in the algorithm, is specified using the data obtained with the use of a simple and easy to use measurement method [22]. The proposed algorithm controls the torque produced by the machine directly to ensure good angular velocity control and dynamical behavior of the drive. In the end, the algorithm is implemented using a fast prototyping card equipped with a Digital Signal Processor (DSP card) and its performance is briefly investigated.

2. Theoretical description of a SynRM drive system

The presented algorithm can be classified as a Direct Torque Control (DTC) algorithm, as during the control system operation an actual value of the electromagnetic torque is estimated and the torque value is controlled using simple PI regulators. This is the standard approach for controlling both asynchronous and synchronous electrical motors [23]. To operate, the proposed control system requires the values of phase currents and the position and angular speed of the rotor of the machine. In general, the proposed algorithm is a modification of the algorithm introduced in earlier work [24].

The general aim of the work is to incorporate a mathematical model of the SynRM machine into the control algorithm, which is described using the Hamilton approach. In such a model, the flux linkage values are treated as state variables, rather than more commonly used current values. This requires the approximation of the multidimensional function that transforms current values into flux linkage values. If such an approximation is known however, the model does not require additional elements to describe nonlinear effects such as magnetic saturation or flux linkage coupling.

If a precise mathematical model is known *a priori*, then incorporating it in the control system allows for some calculations (involving optimal voltage vectors used in the actual working point) to be performed offline and used later as a Look-Up Table (LUT). This simplifies the structure of a control system and lowers the computational time of a one-step algorithm, at the expense of bigger memory usage. Such an algorithm can be also implemented and tested using a fast-prototyping platform (in the research a dSpace card was used), which can be regarded as an advantage.

2.1. Mathematical model of a SynRM machine

The description of the proposed control algorithm should be started with the description of the controlled SynRM. It is assumed that the used machine is three-phase, with the phase windings in wye configuration. With such an assumption its dynamic behavior can be described using the set of equations [21]:

$$\frac{d}{dt} \Psi_{dq} = e_{dq} - R_f i_{dq} (\Psi_{dq}) + p\omega \begin{bmatrix} \Psi_q \\ -\Psi_d \end{bmatrix}, \quad (1)$$

$$\frac{d}{dt} K = T_{em} - T_{load}, \quad (2)$$

$$\frac{d}{dt} \varphi = \frac{K}{I}, \quad (3)$$

where: $\Psi_{dq} = [\Psi_d, \Psi_q]^T$, $i_{dq} = [i_d, i_q]^T$, $e_{dq} = [e_d, e_q]^T$ are the vectors of flux linkages, currents and external voltages in the dq reference frame, R_f is the resistance of the phase winding (assuming equal resistances of the windings), p is the number of pole pairs, ω and φ are the angular velocity and position of the rotor, T_{em} and T_{load} are the electromagnetic and load torque, K is the angular momentum of the rotating masses and I is the moment of inertia of the rotating masses.

The electrical variables are conveniently described in the dq reference frame that rotates with the rotor of the machine [14]. In such a case the relation between currents and flux linkages in the machine is reduced to the vector function $i_{dq} = i_{dq}(\Psi_{dq})$ (called current-flux characteristic later in the paper), that transforms 2-dimensional vectors from the space of flux linkages to the 2-dimensional space of currents. Defined as such, the current-flux characteristic is considered to be independent of the position of the rotor, which omits slotting effects but is a valid assumption when the machine operates at high angular velocity.

In the mathematical model, a simplicial approximation [25] of the current-flux characteristic can be applied. It is based on the sets of corresponding points in the spaces of currents and flux linkages, triangulated (i.e. divided into simplexes, which in 2D spaces are triangles) in the same way, so that corresponding points belong to the matched simplex. Such sets can be obtained with the use of the measurement procedure that is a modification of the current decay test and was formulated in earlier work [22]. The procedure can be performed using relatively simple measurement equipment, leading to the relative uncertainties of the flux measurement equal to approximately 6.5% [26]. The triangulated sets that are the effect of using this procedure for the prototype SynRM are presented in Fig. 2 along with the basic scheme of the approximation. The simplicial approximation can be in fact regarded as the form of a piecewise-affine function.

Using mathematical models (1)–(3), a formula for the electromagnetic torque can be derived:

$$T_{em} = p (\Psi_d i_q - \Psi_q i_d) + \frac{\partial \Psi_d}{\partial \varphi} i_d + \frac{\partial \Psi_q}{\partial \varphi} i_q. \quad (4)$$

In Equation (4) usually the latter 2 terms are omitted, which is dictated by assuming the derivatives $\partial \Psi_d / \partial \varphi$ and $\partial \Psi_q / \partial \varphi$ equal to 0. Considering currents as the functions of flux linkages, Equation (4) plays the key role in the control algorithm formulation.

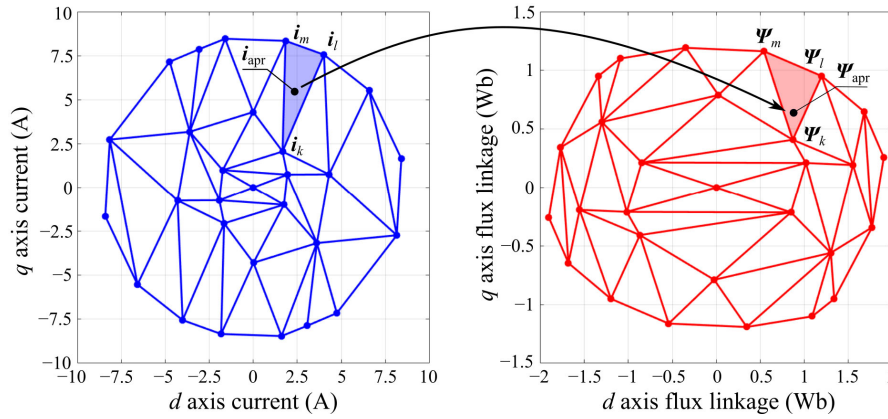


Fig. 2. Triangulated sets of point used in the simplistic approximation

2.2. Strategy for controlling the angular velocity of a SynRM drive

The block scheme of the control algorithm is presented in Fig. 3. The set value of the angular velocity of the rotor is denoted as ω^* . The signal from the PI regulator of the angular velocity is put to the summing node and then on the P regulator of the produced torque, which keeps the system simple. Based on the signal from the torque regulator, a voltage vector is calculated. These calculations, as main part of the algorithm, are thoroughly described below.

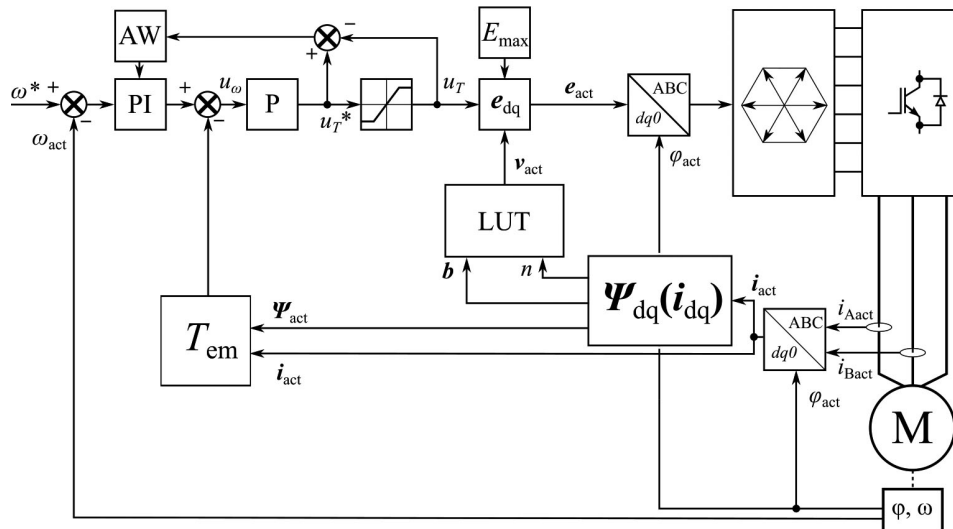


Fig. 3. Block scheme of the proposed control system. n denotes the number of simplex that contains the actual operating point and b is a vector of barycentric coordinates

The algorithm starts with the measurement of the phase current values $i_{A_{act}}, i_{B_{act}}$, the position φ_{act} and the angular velocity ω_{act} of the rotor of the machine. The current value is transformed to

obtain the actual current vector \mathbf{i}_{act} in the dq reference frame. Then the actual value of the flux linkages Ψ_{act} in the dq reference frame is computed. Based on \mathbf{i}_{act} and Ψ_{act} the actual torque value T_{act} is estimated and the regulator signals are computed.

The idea of the voltage vector calculation can be presented assuming a big value of angular velocity error. In such a case the control system should act to reduce this error as fast as possible considering the actual state of the machine and the inverter voltage limit. Hence, the voltage should be set so that it results in the biggest possible change in the torque value in the actual instance of time, to achieve big value angular acceleration of the desired sign (in the desired direction).

The change of torque with respect to time is given by the formula:

$$\frac{dT_{em}}{dt} = \frac{\partial T_{em}}{\partial \Psi_d} \frac{d\Psi_d}{dt} + \frac{\partial T_{em}}{\partial \Psi_q} \frac{d\Psi_q}{dt}. \quad (5)$$

The required partial derivatives can be computed using Equation (4), setting $\partial \Psi_d / \partial \varphi = 0$, $\partial \Psi_q / \partial \varphi = 0$ and considering flux linkages as the state variables. The calculations result in the following formula:

$$\left[\frac{\partial T_{em}}{\partial \Psi_d}, \frac{\partial T_{em}}{\partial \Psi_q} \right]^T = p \left(\begin{bmatrix} i_q \\ -i_d \end{bmatrix} + (\mathbf{\Gamma}_{\text{dyn}})^T \begin{bmatrix} -\Psi_q \\ \Psi_d \end{bmatrix} \right) = \text{grad} (T_{em}(\Psi_{dq})), \quad (6)$$

where $\mathbf{\Gamma}_{\text{dyn}}$ is the inverse matrix of the dynamic inductance matrix in the point of operation on the current-flux characteristic, i.e. $\mathbf{\Gamma}_{\text{dyn}} = \partial \mathbf{i}_{dq} / \partial \Psi_{dq}$. It can be approximated as a matrix that defines the affine function that is valid in the actual simplex containing \mathbf{i}_{act} and Ψ_{act} . With this simplex vertices: $\mathbf{i}_k, \mathbf{i}_l, \mathbf{i}_m$ in the space of currents and Ψ_k, Ψ_l, Ψ_m in the space of flux linkages, this matrix can be computed as:

$$\mathbf{\Gamma}_{\text{dyn}} = \begin{bmatrix} \Psi_k - \Psi_m & \Psi_l - \Psi_m \end{bmatrix}^{-1} \begin{bmatrix} \mathbf{i}_k - \mathbf{i}_m & \mathbf{i}_l - \mathbf{i}_m \end{bmatrix}. \quad (7)$$

Putting (6) and (1) into (5) results in:

$$\frac{dT_{em}}{dt} = \frac{\partial T_{em}}{\partial \Psi_d} (e_d - R_f i_d + p\omega \Psi_q) + \frac{\partial T_{em}}{\partial \Psi_q} (e_q - R_f i_q - p\omega \Psi_d). \quad (8)$$

With maximum length of the voltage vector E_{max} , the external voltages can be written as $e_d = E_{\text{max}} \cos(\theta)$ and $e_q = E_{\text{max}} \sin(\theta)$, with θ being the angle between the chosen vector in the e_{dq} plane and the d axis. Putting this into (8) and calculating the differential of the result with respect to θ yields:

$$\frac{d}{d\theta} \left(\frac{dT_{em}}{dt} \right) = E_{\text{max}} \left(\frac{\partial T_{em}}{\partial \Psi_d} \sin \theta - \frac{\partial T_{em}}{\partial \Psi_q} \cos \theta \right). \quad (9)$$

After setting (8) to be equal to 0, the resulting formula can be used to specify the direction of the voltage vector resulting in the biggest torque change. The unit vector $\mathbf{v}_{\text{max}T}$ of this direction is described in the dq space by the coordinates:

$$\mathbf{v}_{\text{max}T} = \frac{1}{\sqrt{\left(\frac{\partial T_{em}}{\partial \Psi_d} \right)^2 + \left(\frac{\partial T_{em}}{\partial \Psi_q} \right)^2}} \begin{bmatrix} \frac{\partial T_{em}}{\partial \Psi_d} \\ \frac{\partial T_{em}}{\partial \Psi_q} \end{bmatrix}^T. \quad (10)$$

The coordinates of such a vector can be computed for the actual state of the machine, but all the required information is already defined by the obtained sets of points used in the simplicial approximation. Hence, it must be stressed that these calculations can be done offline before the start of the operation of the machine. The vectors can be computed for every point in those sets, so that every vertex of every simplex has a vector assigned to it. Fig. 4 presents those vectors computed for every point of the aforementioned sets, against the set of points in the space of currents. For a given point in the space of currents i_{act} , residing in the found simplex, actual coordinates of an “optimal” vector v_{act} can be calculated using barycentric coordinates, the same that were used to estimate actual flux linkage value Ψ_{act} .

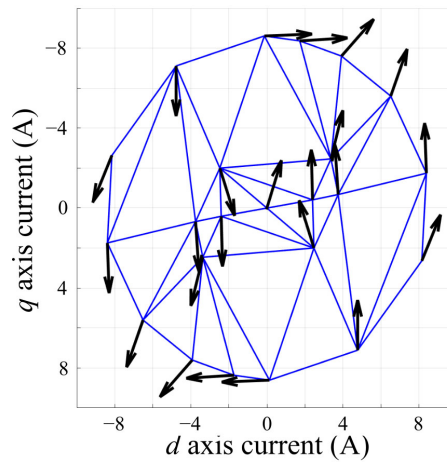


Fig. 4. Calculated directions (black arrows) of the voltage vectors resulting in the biggest torque change

The above description of the algorithm operation assumes big error in angular velocity value, but the direction of the voltage vector, that results in the biggest torque change, does not depend on the actual length of it. This gives the possibility to control the change of torque itself by controlling the length of the voltage vector. Finally, the voltage vector e_{act} produced by the regulator is equal to:

$$e_{act} = E_{max} v_{act} u_T, \quad (11)$$

where u_T is the signal produced by the torque regulator. Based on Equation (10) it is clear that the u_T signal should be bounded (saturated) to not exceed the range from -1 to 1 . This also allows for the implementation of a simple anti-windup filter. The torque regulator signal before saturation u_T^* is equal to:

$$u_T^* = k_T (u_\omega - T_{em}), \quad (12)$$

where u_ω is the signal produced by the angular velocity regulator and k_T is the regulator gain value. The DTC nature of the proposed algorithm is hence directly visible.

3. Implementation of the drive system

3.1. Laboratory stand and the controlled machine

The general block diagram of the created prototype SynRM drive system is presented in the Fig. 5.

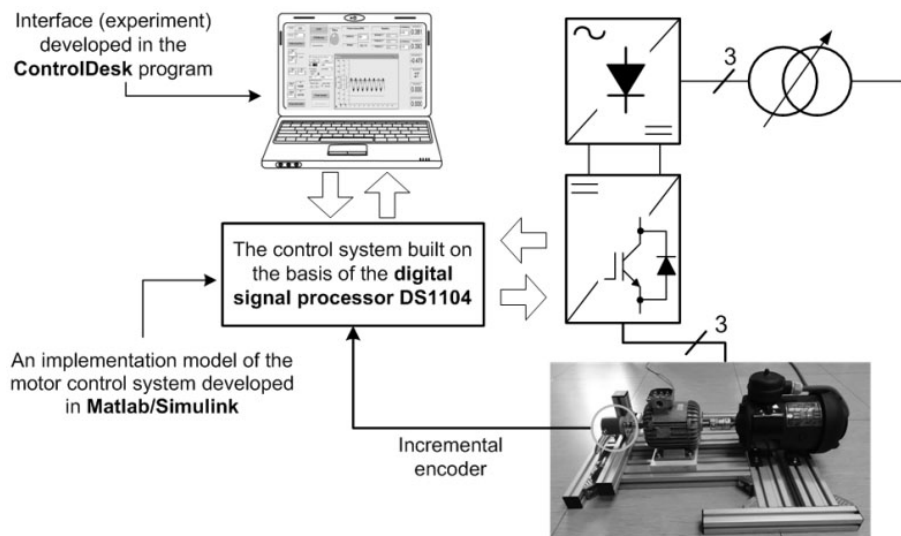


Fig. 5. General block diagram of the drive system

The main part of the system is a DSP card that realizes the proposed control algorithm. The processor cooperates with the 3-phase inverter, build of three half-bridges made of insulated gate bipolar transistors (IGBTs). The current in the windings of the machine was measured using LEM LA50 transducers, and the angular position and velocity of the rotor were measured using an incremental encoder. The controlled SynRM machine is a prototype motor incorporating the classical designed rotor and stator, presented in Figs. 1(a) and 1(b). To load the controlled machine, a DC generator was used. The value of the resistance, that was connected to the terminals of the generator was constant and the load torque was changed by changing the current of the field winding.

3.2. Implementation of the control algorithm in Matlab/Simulink environment

As already stated, the dSpace card DS1104 was used during the implementation of the control algorithm. This allows for building the control system as a block diagram in the MATLAB/Simulink environment. The scheme of it is presented in Fig. 6.

The hardware components of the DSP card, such as analog-to-digital converters, a PWM module and the counter that handles the signal from encoder, were maintained using standard library blocks. The currents and angular velocity signals were filtered using simple averaging filters.

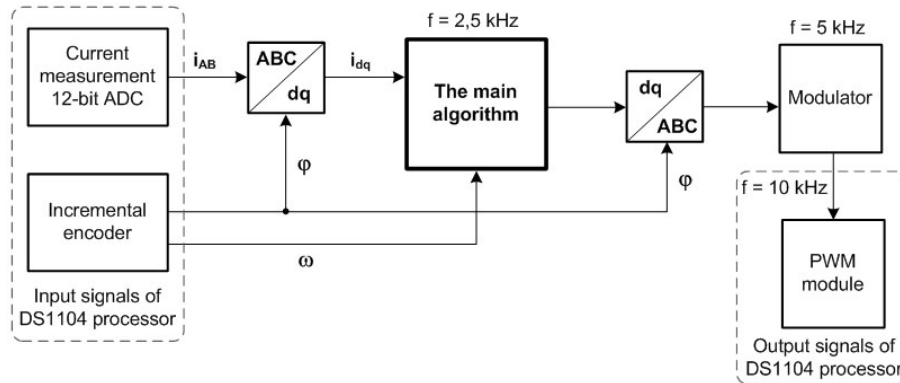


Fig. 6. Block diagram of the control algorithm loaded to the DSP

The main parts of the algorithm, including $dq0$ transforms, a voltage modulator and the required calculations, were implemented using “S-Function Builder” blocks. The algorithm can be then implemented using the C language, which is much more convenient and flexible than implementing it with the use of simple blocks from the MATLAB library.

4. Prototype SynRM drive test

To examine the drive operation, four tests were executed. During the tests the maximum available voltage was set to $E_{\max} = 340$ V. The acquired time plots of the angular velocity are presented in Fig. 7. The tests are summarized in Table 1.

Table 1. Summary of the drive tests

Fig. no	Test description	Additional notes
7(a)	Startup and sudden change in loading torque value at 1.5 s	–
7(b)	Sudden change in set angular velocity value	Loading torque proportional to angular velocity
7(c)	Consecutive startups “on the fly” (with non-zero velocity)	–
7(d)	Operation with saturated controller	Loading torque proportional to angular velocity, above the maximum achievable torque for the set value of the angular velocity

Generally, it can be observed that in the dynamic states the operation of the drive is satisfactory. During the tests the load torque was set so that in the steady state the core of the machine was

saturated and such a situation is well-handled by the controller of the drive. However, one drawback of the formulated algorithm is that the operating point of the machine in the steady state (i.e. obtained values of currents and flux linkages) was far from the point on maximum efficiency considering the set values of load torque and the set angular velocity. Such behavior was observed during all tests.

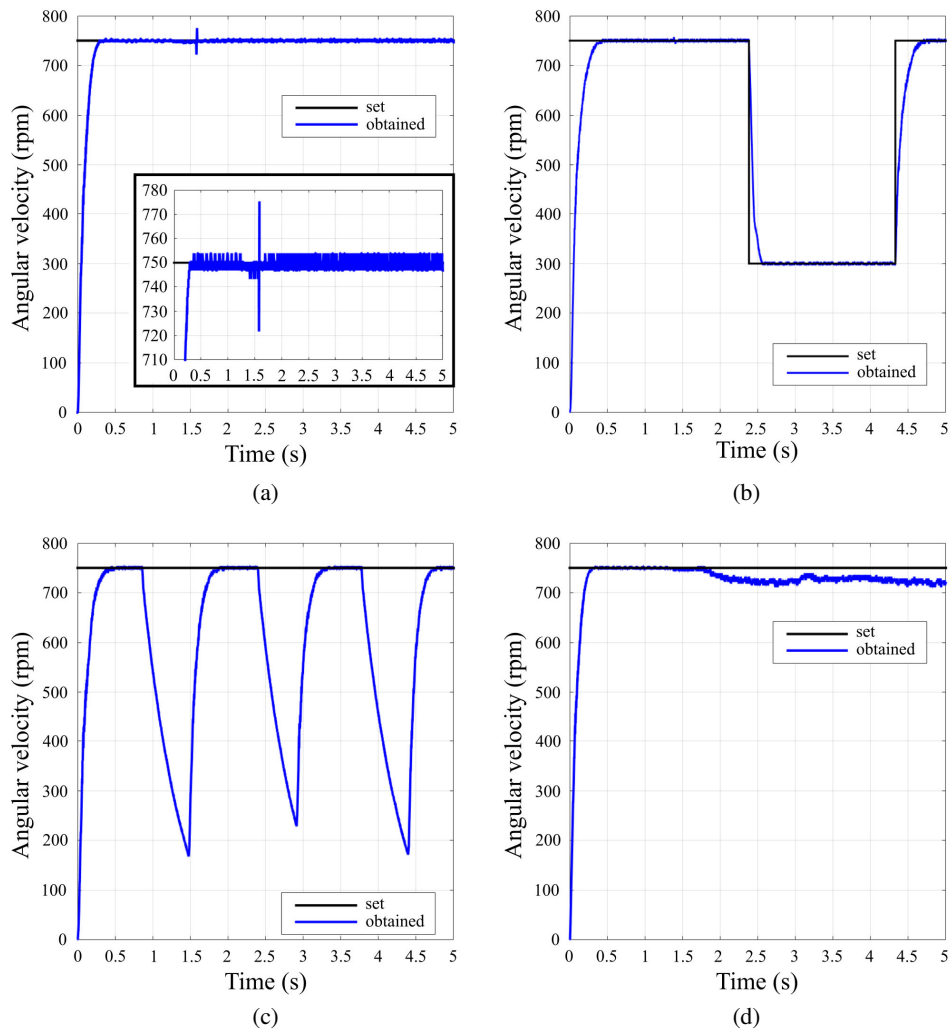


Fig. 7. Time plots of angular velocity acquired during testing of the prototype SynRM drive

5. Conclusions

In the paper a drive system containing the classical SynRM is described. In the system the angular velocity is controlled by direct control of the electromagnetic torque produced by

the machine. The used control algorithm is based on the mathematical model of the electrical machine, described using Hamilton formalism. The key part of this model is the approximation of the current-flux characteristic, which is based on the data obtained by measurement. The gathered data are then used to compute the optimal voltage vector direction for every region of the useful operating range of the machine (either in the space of currents or flux linkages). These computations can be done offline (not during actual work of the drive) and passed to the drive controller as a look-up table. This decreases the amount of calculations that have to be done at every step of the control algorithm.

The proposed algorithm was implemented in the prototype drive system with the use of a DSP card. After implementing, the drive system operation was briefly examined. The tests show generally good control quality, with an algorithm capable of controlling the angular velocity under rapid load changes, rapid changes of demanded angular velocity and capable of executing start on-the-fly.

Despite the positive results, the drawback of the algorithm is that it does not optimize the working point with regard to the drive efficiency after the stable state is reached. This is because the algorithm was generally prepared to quickly reduce very large control errors. The algorithm should be hence extended by procedures for achieving a better operating point when the control error is small. One such possibility is to calculate the voltage value in every step of the algorithm not only to modify the value of the produced torque (as presented), but also to push the operating point of the drive, as seen in the space of currents, towards the so called Most Torque Per Ampere (MTPA) curve, i.e. the curve consisting of points in which the value of the produced torque is the biggest regarding their distance from the (0, 0) point of the space of currents.

At this stage of research the presented drive was designed to investigate the possibility of defining its control algorithm based on the Hamiltonian model of the machine, with flux linkage value approximated simplistically. The presented approach was proven to be promising, but could not be directly used in practice. The reason is that it does not ensure high efficiency of the drive, which is one of the main advantages of a SynRM. Further improvements in the drive system and the used algorithm will be done in the future research to overcome this weakness.

References

- [1] Boglietti A., Pastorelli M., *Induction and synchronous reluctance motors comparison*, IECON Proceedings of Industrial Electronic Conference, pp. 2041–2044 (2008).
- [2] Kärkkäinen H., Aarniovuori L., Niemelä M., Pyrhönen J., Kolehmainen J., *Technology comparison of induction motor and synchronous reluctance motor*, Proceedings of IECON 2017 – 43rd Annual Conference IEEE Industrial Electronics Society, no. 640, pp. 2207–2212 (2017).
- [3] Rettinger F., Huth G., *Variable-speed PM synchronous motors with ferrite excitation*, Electrical Engineering, vol. 99, no. 2, pp. 639–648 (2017).
- [4] Taghavi S., Pillay P., *A core analysis of the synchronous reluctance motor for automotive applications*, Proceedings of 2014 International Conference on Electrical Machines (ICEM) 2014, pp. 961–967 (2014).
- [5] De Gennaro M. et al., *Designing, prototyping and testing of a ferrite permanent magnet assisted synchronous reluctance machine for hybrid and electric vehicles applications*, Sustainable Energy Technologies and Assessments, vol. 31, pp. 86–101 (2019).

- [6] Widmer J.D., Martin R., Kimiabeigi M., *Electric vehicle traction motors without rare earth magnets*, Sustainable Materials Technologies (2015).
- [7] Kerdsup B., Fuengwarodsakul N.H., *Performance and cost comparison of reluctance motors used for electric bicycles*, Electrical Engineering, vol. 99, no. 2, pp. 475–486 (2017).
- [8] Kostko J.K., *Polyphase reaction synchronous motors*, Journal of the American Institute of Electrical Engineers, vol. 42, no. 11, pp. 1162–1168 (1923).
- [9] Boldea I.G., *Reluctance Synchronous Machines and Drives*, Oxford: Oxford University Press (1996).
- [10] Jurca F.N., Inte R., Martis C., *Optimal rotor design of novel outer rotor reluctance synchronous machine*, Electrical Engineering, pp. 1–10 (2019).
- [11] Park J.M., Il Kim S., Hong J.P., Lee J.H., *Rotor Design on Troque Ripple Reduction for a Synchronous Reluctance Motor With Concentrated Winding Using Response Surface Methodology*, vol. 42, no. 10, pp. 3479–3481 (2006).
- [12] Jurca F.N., Ruba M., Martis C., *Design and control of synchronous reluctances motors for electric traction vehicle*, 2016 International Symposium on Power Electronics and Electric Drives, Automation Motion, SPEEDAM 2016, pp. 1144–1148 (2016).
- [13] Richter J., Gemasmer T., Doppelbauer M., *Predictive current control of saturated cross-coupled permanent magnet synchronous machines*, 2014 International Symposium on Power Electronics Electrical Drives, Automation and Motion, SPEEDAM 2014, pp. 830–835 (2014).
- [14] Park R.H., *Two-reaction theory of synchronous machines generalized method of analysis-part I*, Transactions of the American Institute of Electrical Engineers, vol. 48, no. 3, pp. 716–727 (1929).
- [15] Chu C.T., Chiang H.K., Chung K.C., Lin T.C., *Self-tuning single input fuzzy controller for a synchronous reluctance motor*, 2014 International Symposium Next-Generation Electronics ISNE 2014, vol. 4, no. 3, pp. 4–7 (2014).
- [16] Choi J.S., Park K.T., Chung D.H., Ko J.S., Park B.S., *Efficiency optimization control of SynRM drive by LM-FNN controller*, 7th International Conference on Power Electronics ICPE'07, pp. 373–377 (2008).
- [17] Matsuo T., Lipo T.A., *Field oriented control of synchronous reluctance machine*, Proceedings of IEEE Power Electronics Specialist Conference – PESC '93, pp. 425–431 (1993).
- [18] Morales-Caporal R., Pacas M., *A predictive torque control for the synchronous reluctance machine taking into account the magnetic cross saturation*, IEEE Transactions on Industrial Electronics, vol. 54, no. 2, pp. 1161–1167 (2007).
- [19] Wróbel K.T., Szabat K., Serkies P., *Long-horizon model predictive control of induction motor drive*, Archives of Electrical Engineering, vol. 68, no. 3, pp. 579–593 (2019).
- [20] Hanamoto T., Ghaderi A., Fukuzawa T., Tsuji T., *Sensorless control of synchronous reluctance motor using modified flux linkage observer with an estimation error correct function*, in Recent Developments of Electrical Drives, Springer, pp. 155–164 (2006).
- [21] Bugsch M., Piepenbreier B., *HF Test Current-Ripple-Control-Based Sensorless Method for SynRMs in the Low- and Zero-Speed Range Leading to an Adaptive Square-Wave-Shaped Voltage Injection*, 2018 IEEE 9th International Symposium on Sensorless Control Electrical Drives, SLED 2018, pp. 24–29 (2018).
- [22] Burlikowski W., *Hamiltonian model of electromechanical actuator in natural reference frame. Parts 1 & 2*, Archives of Electrical Engineering, vol. 60, no. 3, pp. 317–348 (2011).
- [23] Burlikowski W., Kielan P., Kowalik Z., *Measurement based determination of the current-flux characteristic of a synchronous reluctance machine using a standard 3-phase inverter and a digital signal processor*, in AIP Conference Proceedings, vol. 2029, iss. 1 (2018), DOI: 10.1063/1.5066471.

- [24] Vas P., *Sensorless Vector and Direct Torque Control*, (Monographs in Electrical Electronic Engineering, Oxford University Press, USA, p. 768 (1998).
- [25] Burlikowski W., Kohlbrenner L., Kowalik Z., *Hamiltonian model based control algorithm for electromechanical actuator*, in 2017 International Symposium on Electrical Machines, SME 2017 (2017).
- [26] Vick J.W., *Homology Theory: An Introduction to Algebraic Topology*, New York: Springer (1994).
- [27] Kowalik Z., *Uncertainty of the magnetic flux linkage measurements performed by modified current decay test*, Archives of Electrical Engineering, vol. 66, no. 3 (2017).